

# A Method of Image-Based Aberration Metrology for EUVL Tools

Zac Levinson, Bruce W. Smith  
Rochester Institute of Technology

Sudhar Raghunathan, Erik Verduijn, Obert Wood, Pawitter  
Mangat  
GLOBALFOUNDRIES

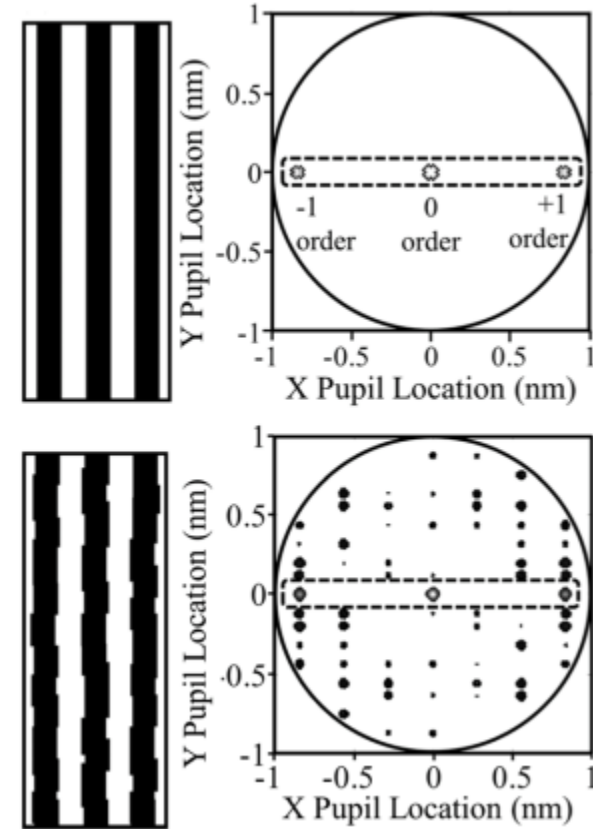
Kenneth Goldberg, Markus Benk, Antoine Wojdyla  
Lawrence Berkeley National Laboratory

Vicky Philipsen, Eric Hendrickx  
IMEC



# Introduction

- Pupil plane characterization continues to play a critical role in image process optimization moving into EUVL
- Additional importance in understanding the influence and variations of aberrations during system use
- At RIT we have developed a method to measure optical aberrations of EUVL systems from images formed by that system



(Baylav et al., 2013)

# Introduction

- Past studies, and traditional aberration theory in general, have focused on evaluation of pupil phase variation
- Other system variations have been assumed to be small, but are potentially more important in EUV imaging.
- We examine the flexibility of an image-based method using two experimental case studies:
  - 1) Pupil phase variation of an ASML NXE:3100 exposure system using SEM image analysis through inverse solutions
  - 2) Amplitude *and* phase pupil variation in the SEMATECH High-NA Actinic Reticle review Project (SHARP)—an EUV mask microscope at Lawrence Berkeley National Laboratory



# Outline

- Modeling pupil variation
- Image-based method for pupil variation extraction
- Extraction of pupil amplitude variation
- Image-based metrology experiments
- Concluding remarks



# Modeling Pupil Variation

The transfer of light through an optical system in the frequency domain can be given by:

$$\widetilde{E}_i(u, v) = \widetilde{E}_o(u, v) \cdot P(u, v)$$



# Modeling Pupil Variation

The transfer of light through an optical system in the frequency domain can be given by:

$$\widetilde{E}_i(u, v) = \widetilde{E}_o(u, v) \cdot P(u, v)$$

The pupil function is complex-valued, so it can be expressed as magnitude and phase:

$$P(u, v) = \alpha(u, v)e^{i\phi(u, v)}$$



# Modeling Pupil Variation

The transfer of light through an optical system in the frequency domain can be given by:

$$\widetilde{E}_i(u, v) = \widetilde{E}_o(u, v) \cdot P(u, v)$$

The pupil function is complex-valued, so it can be expressed as magnitude and phase:

$$P(u, v) = \alpha(u, v)e^{i\phi(u, v)}$$

The phase function is expanded in a Fourier-Zernike series:

$$W(u, v) = \sum_{n=0}^{\infty} a_n Z_n(\rho, \theta)$$



# Modeling Pupil Variation

The transfer of light through an optical system in the frequency domain can be given by:

$$\widetilde{E}_i(u, v) = \widetilde{E}_o(u, v) \cdot P(u, v)$$

The pupil function is complex-valued, so it can be expressed as magnitude and phase:

$$P(u, v) = \alpha(u, v)e^{i\phi(u, v)}$$

The phase function is expanded in a Fourier-Zernike series:

$$W(u, v) = \sum_{n=0}^{\infty} a_n Z_n(\rho, \theta)$$

We define the amplitude in terms of a slight perturbing function:

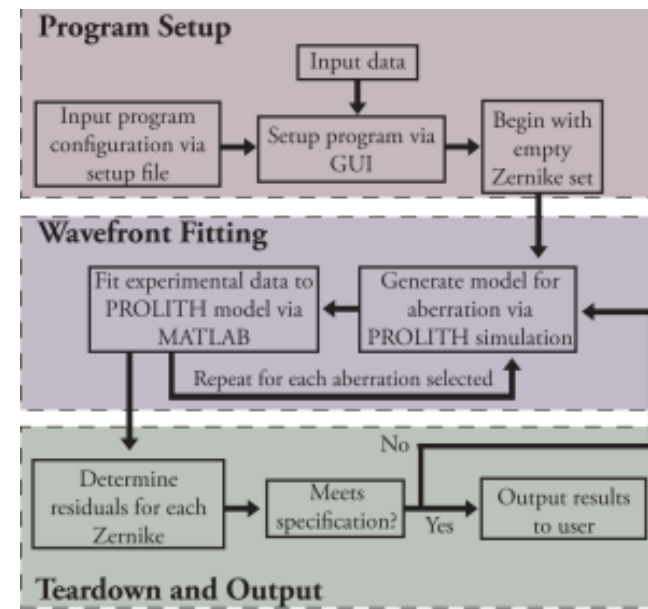
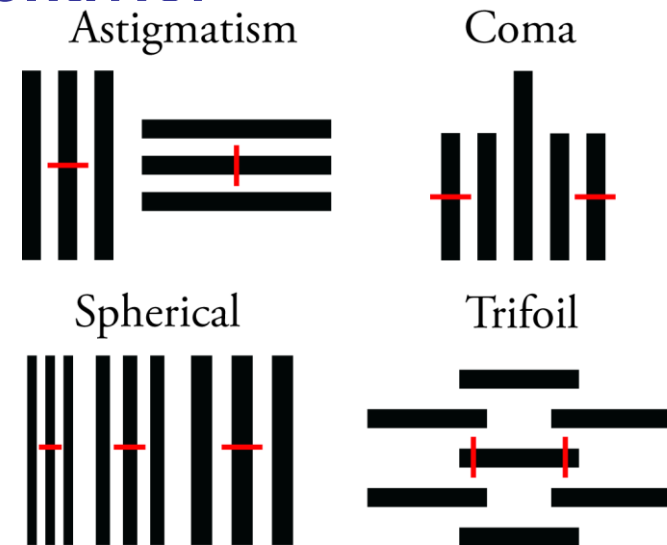
$$\alpha(\rho, \theta) = \begin{cases} 1 + A(\rho, \theta) & : \rho \leq 1 \\ 0 & : \rho > 1 \end{cases}$$



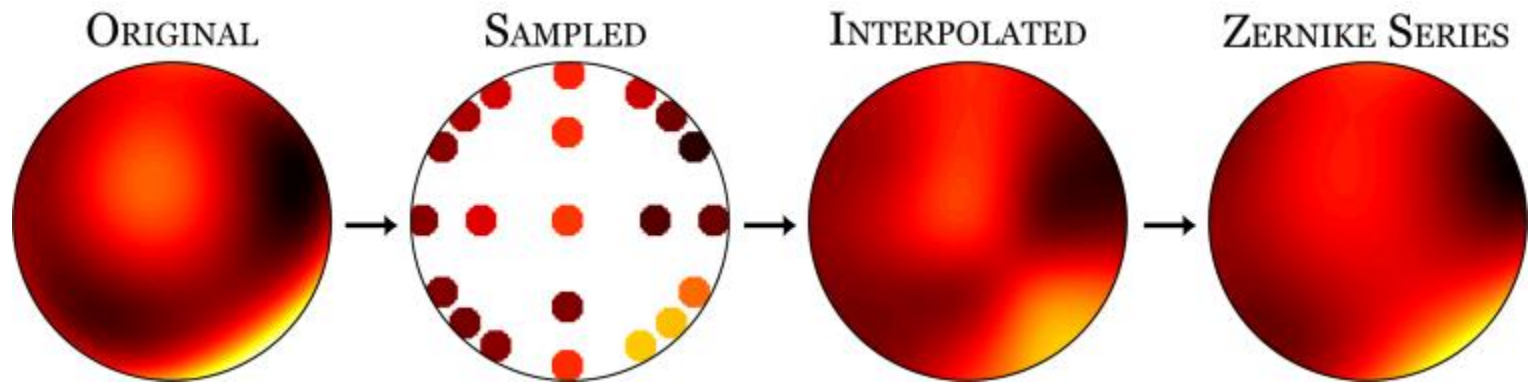
# Image-Based Method

Automated, iterative, model-based solutions to particular image behavior

- Aberrations measured via targets sensitive to specific aberrations
- Input data as CD or aerial image
- Provides in-situ aberration monitoring
- All targets need to be optimized for each tool/illumination
- Targets are generally available on existing reticles
- Has been demonstrated in the past for pupil phase extraction



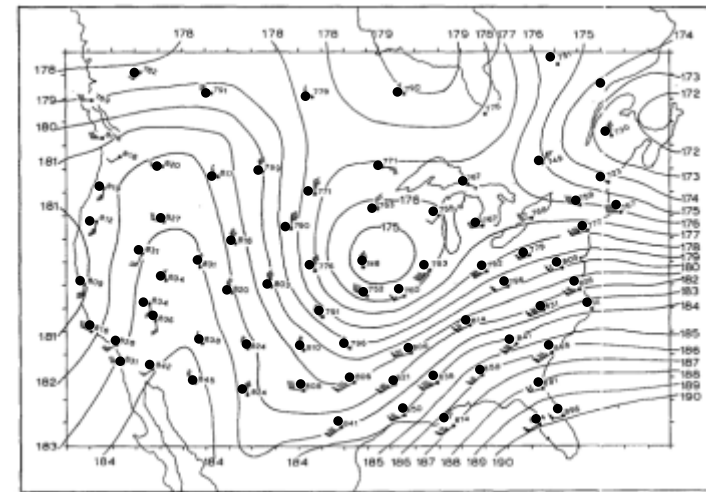
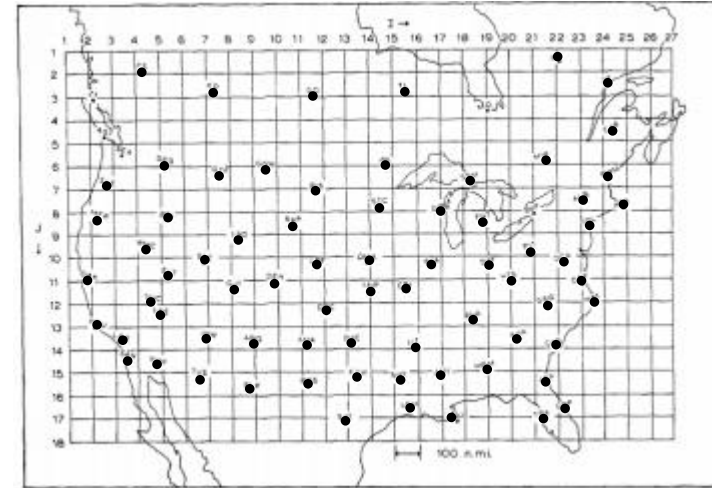
# Extraction of Pupil Amplitude Variation



- A partially coherent source samples the pupil function *and* averages across the source
- Aerial image simulations iteratively fit to determine source-average sample value
- Barnes objective analysis is used to interpolate across the pupil between samples

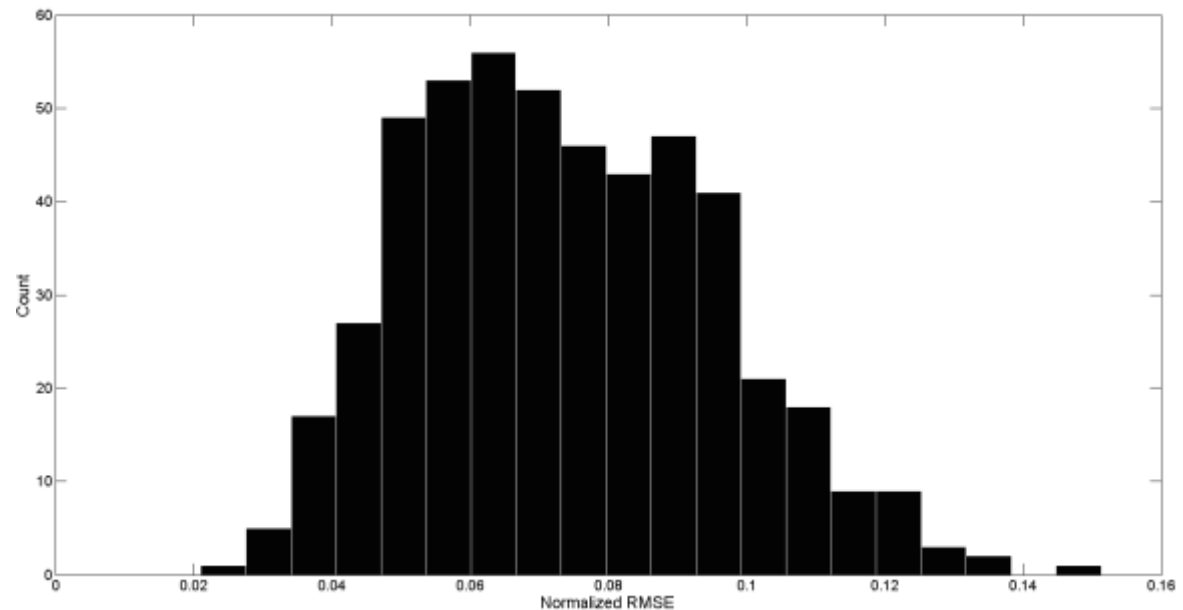
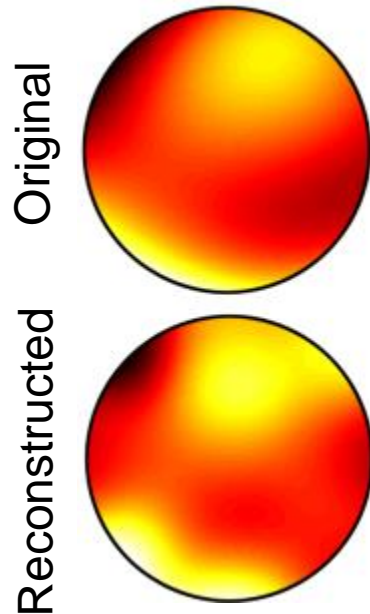
# Barnes Objective Analysis

- Commonly used in meteorological modeling
- Uses an initial guess for each grid point, then iteratively corrects it based on error computed from known values
- Weight of each error is inversely proportional to its distance from other points
- Highly accurate even when the samples are disordered and/or unevenly spaced



(Barnes, 1964)

# Extraction of Pupil Amplitude Variation



- 500 random amplitude functions comprised of third-order Zernike amplitude polynomials ( $Z_A5$ - $Z_A11$ ) sampled in  $\rho=0.5$  and  $\rho=0.9$  pupil zones with  $0.1\sigma$  source
- Residuals are  $\chi^2$  distributed with a mean around 6%

**Can reproduce the original function with little error from a small number of samples**

# Extraction of Pupil Amplitude Variation

- The original functions were made of Z5-Z11, but higher order terms appear in the reconstruction
- Blurring can be reduced by increasing the source coherence and the number of samples
- Function can still be represented with low error in less than 36 terms (~6% NRMSE)
- Expansion in the first 36 combinations of Cartesian Legendre polynomials would require more terms

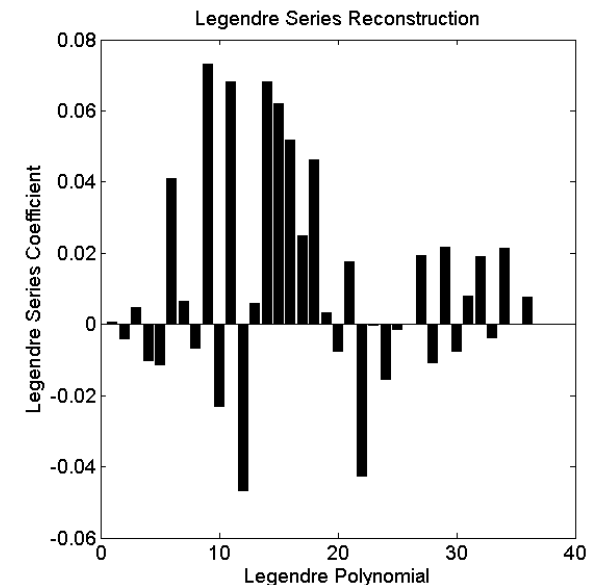
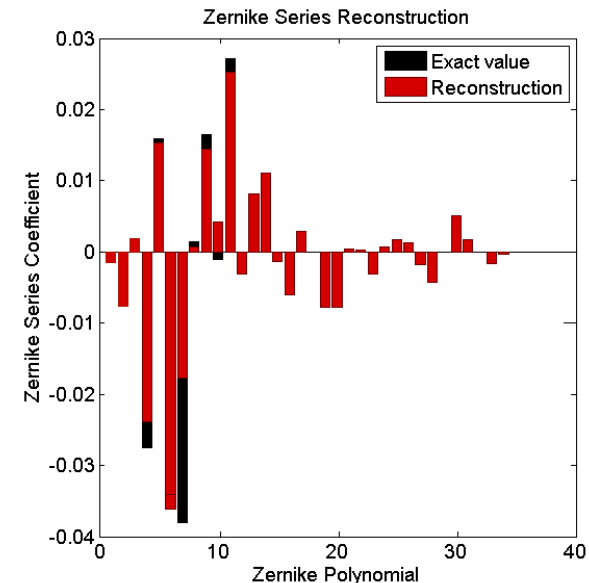
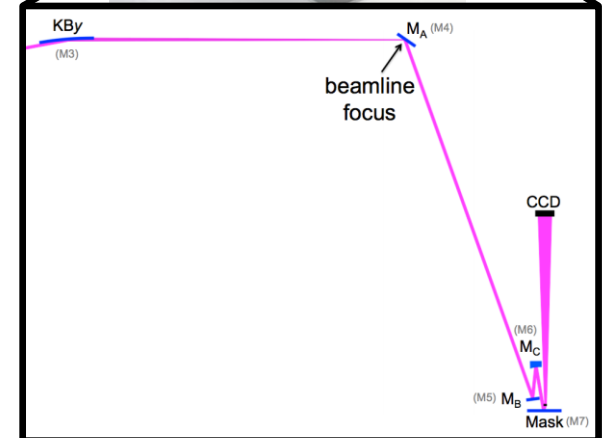
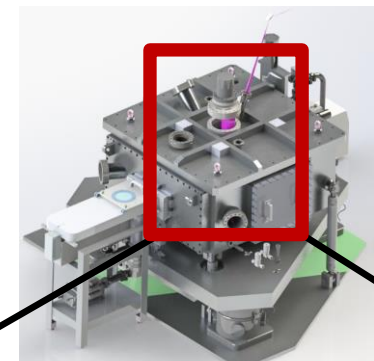


# Image-Based Metrology Experiments

- ASML NXE:3100 Scanner
  - Full field catoptric lens
  - Fixed set of illuminators at 0.25NA
  - CD from SEM micrograph of resist patterns
- SEMATECH Actinic Reticle Review Project (SHARP)
  - Zone plate lens (0.25-0.625 4xNA)
  - Free form sources available by using MEMs mirror
  - Aerial image captured as CCD images



# Dominant Sources of Aberration: NXE3100 vs. SHARP

## NXE:3100

- Mask defectivity
- Multilayer mirror defectivity
- Each multilayer mirror reflection
- Thermal shifting

## SHARP

- Mask defectivity
- Multilayer mirror defectivity
- Zone plate lens
- Beam set-up/system alignment
- Thermal shifting



# NXE:3100 Target Selection

## Inputs

- Annulus 0.5/0.8 at 0.25 NA
- +75 nm focus offset

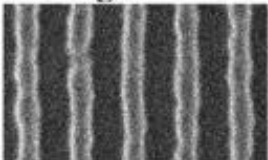
## Constraints

- NILS threshold of 2.0
- Aberration tolerance of mean ADT values

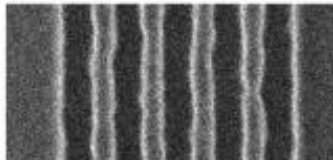
## Optimized targets

- 32 nm line/space array (astigmatism)
- 30 nm 5-bar (coma)
- 26 nm line through pitch (spherical)
- 35 nm t-bar (trefoil)

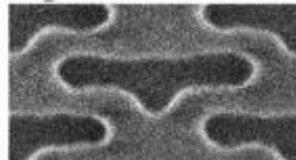
Astigmatism



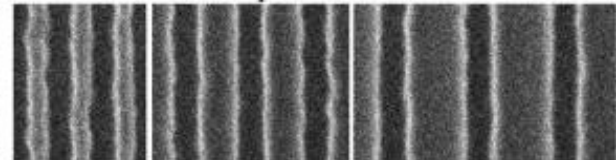
Coma



Trefoil



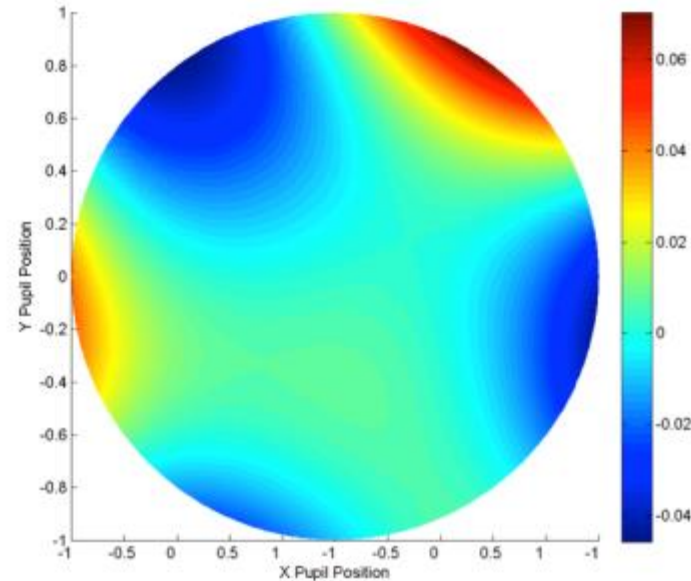
Spherical





# NXE:3100 Wavefront Extraction

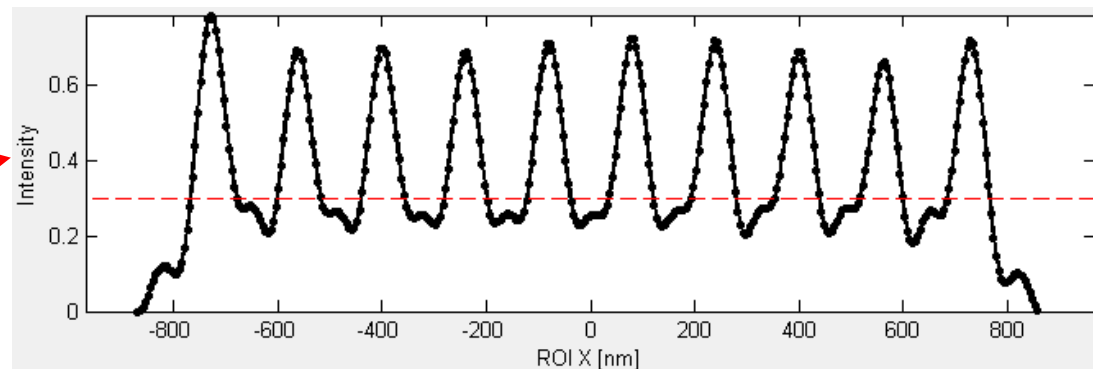
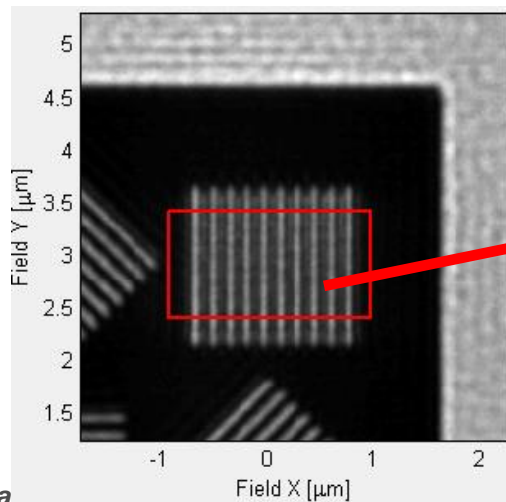
- Extracted NXE:3100 pupil phase variation
- CDs measured via custom offline metrology code
- 10 iterations were necessary to converge on a solution (~20 minute runtime)
- RMS of  $13.4m\lambda$  or 0.181 nm
- $\Delta$ CD MSE is the error in the analytical  $\Delta$ CD model



Aberration Name	Extracted Value [ $m\lambda$ ]	$\Delta$ CD Mean Square Error [ $nm^2$ ]
Astigmatism 90°	-0.82	0.136
Astigmatism 45°	+26.58	0.184
Coma X	-2.92	0.038
Coma Y	+12.00	0.043
Spherical	+0.15	N/A
Trefoil X	-36.09	1.032
Trefoil Y	+1.27	0.590

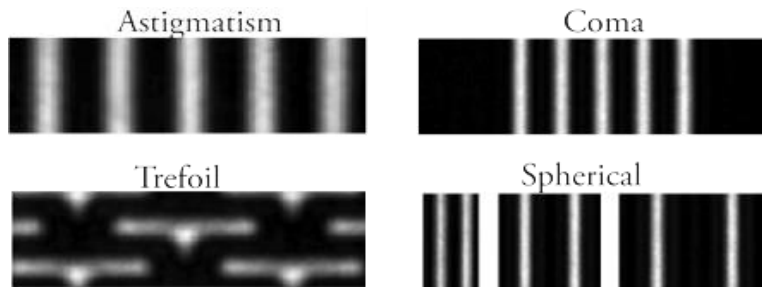
# SHARP Target Selection

- Very low partial coherence available ( $\sigma=0.1$  used)
- Records gray levels, so modulation is less important
- Accomplished by calculating the size/orientation required to sample the desired pupil locations ( $\rho=0.5$  and  $\rho=0.9$  pupil zones)
- Images were analyzed in custom image processing code



# SHARP Target Selection

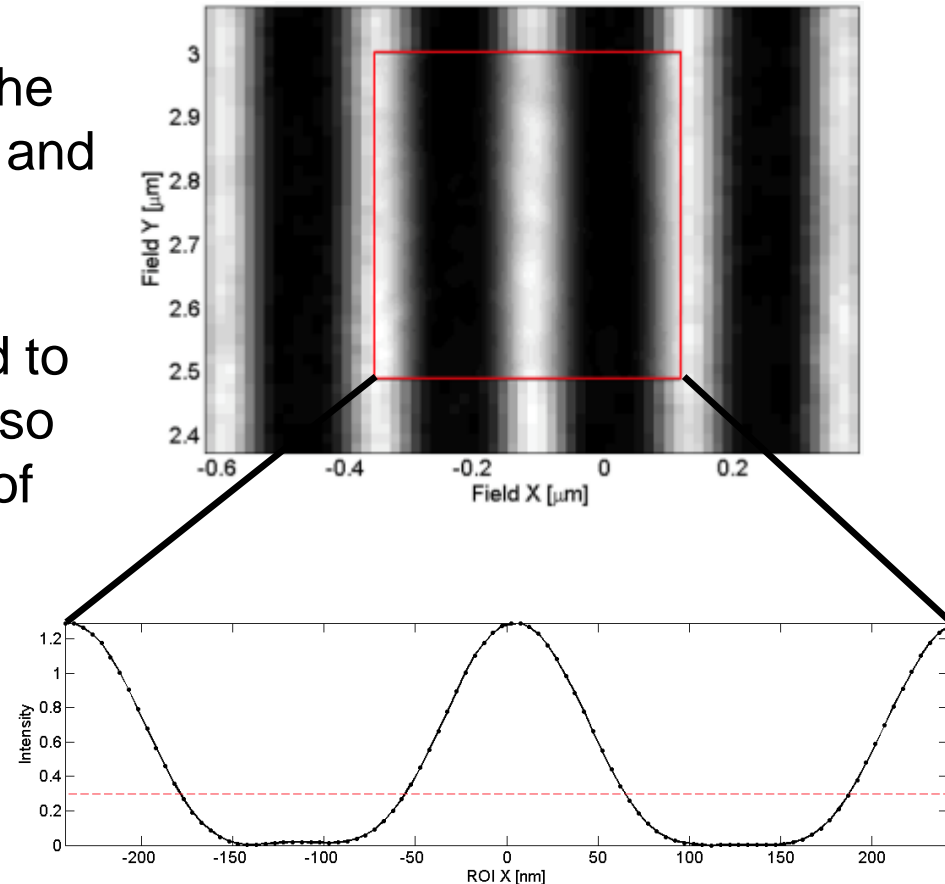
- Very low partial coherence available ( $\sigma=0.1$  used)
- Records gray levels, so modulation is less important
- Accomplished by calculating the size/orientation required to sample the desired pupil locations ( $\rho=0.5$  and  $\rho=0.9$  pupil zones)
- Images were analyzed in custom image processing code



Aberration Name	Structure Type	Target CD [nm]
Astigmatism 90°	Vertical/Horizontal Line/Space	30
Astigmatism 45°	45°/135° Line/Space	30
Coma X	Vertical 5-bar	50
Coma Y	Horizontal 5-bar	50
Spherical	Line through pitch	30
Trefoil X	Horizontal T-Bar	35
Trefoil Y	Vertical T-Bar	35

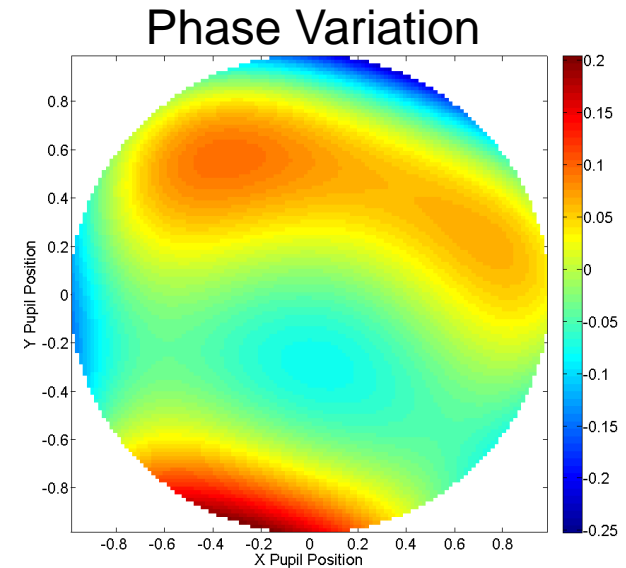
# SHARP Image Processing

1. Dark current noise from the CCD was subtracted from the images, then slight rotation and alignment errors were corrected
2. The image was interpolated to a higher pixel grid, which also deconvolves the response of the CCD sensor
3. The interpolated region was averaged column-wise and normalized to obtain an approximate aerial image



# SHARP Wavefront Extraction

- Pupil amplitude *and* phase variation was extracted
- 8 iterations were necessary to converge on a solution (18 hour runtime)
- Pupil *phase* RMS of  $61.3\text{m}\lambda$  or  $0.828\text{nm}$
- Pupil *amplitude* RMS of 10.18%

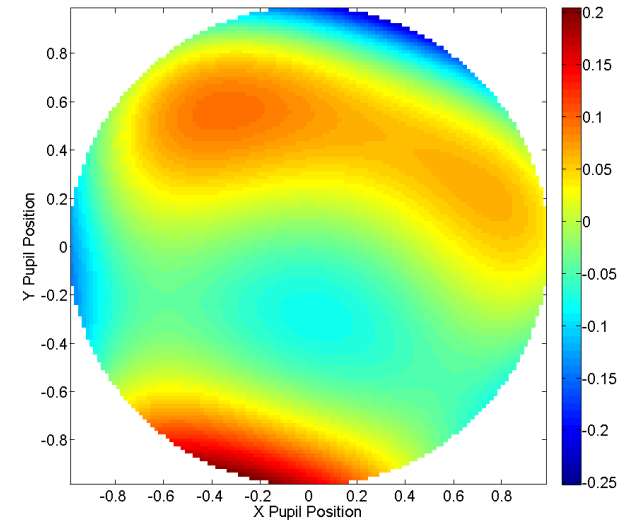


Aberration Name	Extracted Value [ $m\lambda$ ]
Astigmatism $90^\circ$	-18.32
Astigmatism $45^\circ$	-1.20
Coma X	-6.56
Coma Y	-118.55
Spherical	-39.65
Trefoil X	+67.97
Trefoil Y	+92.16

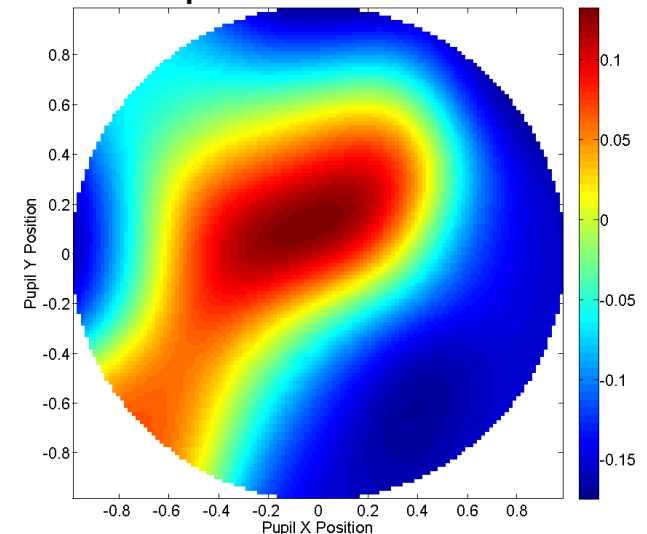
# SHARP Wavefront Extraction

- Pupil amplitude *and* phase variation was extracted
- 8 iterations were necessary to converge on a solution (18 hour runtime)
- Pupil *phase* RMS of 61.3mλ or 0.828nm
- Pupil *amplitude* RMS of 10.18%

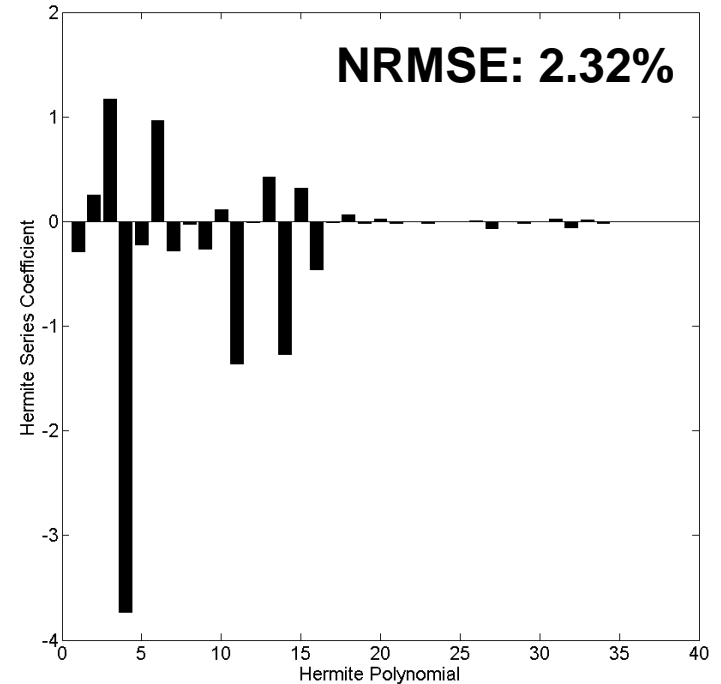
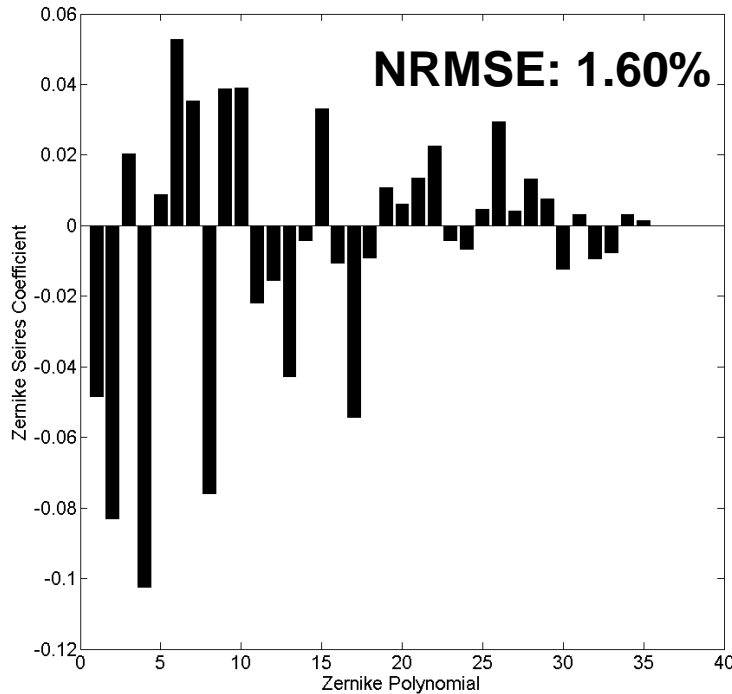
Phase Variation



Amplitude Variation



# SHARP Amplitude Expansions



- By visual inspection the amplitude appears to vary primarily around zero-frequency
- Amplitude function expanded in Zernike polynomials and Hermite polynomials
- Most Zernike polynomials are zero at the origin, so Hermite polynomials provide the better expansion

# Concluding Remarks

- Developing framework for pupil amplitude and phase extraction via image data
- Tested experimentally using NXE:3100 EUV scanner and SHARP EUV microscope
- Hermite polynomials appear to provide better fit to pupil amplitude variation than Zernike polynomials
- NXE:3300 exposures planned
- Future work will focus on studying pupil amplitude variation further and reducing runtime





# Acknowledgments

The authors would like to thank:

- Semiconductor Research Corporation (SRC) / Global Research Collaboration (GRC) through Research Task 2126.001
- KLA Tencor for the use of PROLITH™ lithography simulator

